# Chapter 8
# Nanoparticles-Emerging Contaminants

**Emma J.E. Stuart and Richard G. Compton**

## 8.1 Introduction: Nanoparticles in the Environment and the Need for Monitoring

A nanoparticle is widely considered to be a particle with at least one dimension that is less than 100 nm as reflected in the IUPAC definition[1] that a nanoparticle is a "microscopic" particle, often restricted to the so-called nanosized particles. The definition partially overlaps that of colloids which are dispersions in a fluid medium of particles between 1 nm and 1 μm in size. More usefully the term "nanoparticle" often implies a particle of sufficiently small size in contrast to bulk media of the same chemical composition such that one or more of its properties—optical, electronic, mechanical, . . .—is size dependent.

Environmental nanoparticles primarily originate from natural sources or from human manufacturing activities. The former includes particles from forest fires or volcanic emissions and some of those made of humic materials as well as biological particles such as bacteria and viruses. The incidence of manufactured nanoparticles reflects the huge growth in the nanotechnology industries in recent years with continued expansion expected such that the US National Science Foundation predicts a global $1 trillion market with two million workers in the nanotechnology area by 2015[2] with broad and diverse applications in materials science, medicine, energy, communication and the environment.[3] Nanomaterials feature in consumer products such as electronic components, cosmetics, cigarette filters, antimicrobial and stain-resistant fabrics,[3] more specifically as batteries, skin-care products, paints, wound dressings, food additives, toothpastes, etc.[4] Indeed no less than ca. 15 % of all global consumer products are estimated to be "nano-enabled".[5] Nanoparticles have also been employed in environmental remediation to improve

E.J.E. Stuart • R.G. Compton (✉)
Department of Chemistry, Oxford University, Oxford, United Kingdom
e-mail: emma.stuart@hertford.ox.ac.uk; richard.compton@chem.ox.ac.uk



L.M. Moretto, K. Kalcher (eds.), *Environmental Analysis by Electrochemical Sensors and Biosensors*, DOI 10.1007/978-1-4939-1301-5_8

the quality of air, water and soils. The US Environmental Protections Agency (EPA) allocated $1 billion for environmental remediation in 2009.[3,6] As an illustration magnetic iron oxides have been used to remove arsenic from drinking water. The ions adsorb on the nanoparticle surface and then a magnetic field is used to separate the complex from the water.[7] Gold nanoparticles supported on alumina have been used to remove inorganic mercury from drinking water[8] whilst iron nanoparticles have been used to remove metals such as Cr(VI), U(IV and VI) and Co(II).[9–11] The latter have also been used to degrade organic pollutants as have $TiO_2$ nanoparticles.[2]

"Incidental nanoparticles" are produced as a side product of anthropogenic processes such as in automobile exhausts. One interesting but unexpected source of incidental nanoparticles relates to the discovery[12] that silver and copper metallic nanoparticles are formed spontaneously on the surface of manmade objects (made of Ag and Cu) that humans have long been in contact with and that macroscale objects represent a potential source of nanoparticles in the environment.

The most important environmental nanoparticles are carbon nanotubes (CNTs), fullerenes (such as $C_{60}$), nanowires, $TiO_2$, ZnO, $CeO_2$, $SiO_2$ (silica), iron oxides, alumina, hydroxyapatite and metallic nanoparticles such as Fe, Ag and Au.[4] World production of $TiO_2$ is estimated to be in excess of 40,000 tons per annum with most of the material being nano-sized.[13]

Because of their size nanoparticles can display significantly changed behaviour in comparison with the corresponding macroscopic materials. Most notably the reduced size leads to high surface area-to-volume ratios, high absolute surface areas and changed electronic properties arising from quantum effects leading to changed chemical and physical properties such as[3] aggregation, electrical conductivity, heat conduction, catalytic activity, surface chemistry, mechanical strength and solubility.

An implication of the changed reactivity between the macro- and nanoscale is that the documentation and understanding of the effects of nanoparticles on human health as well as on plants and other animals are at a relatively immature stage. There is evidence that nanoparticles are usually more toxic than larger particles of the same material.[14,15] Origins of some nanotoxicity have been suggested to lie in the ability of for example Fe nanoparticles to generate radical species, coupling into the chemistry of reactive oxygen species and the generation of oxidative stress or removal of antioxidants.[16] In other cases the changed physical and chemical properties from the macroscale can make materials behave quite differently from the bulk analogs. In some cases positive effects, for example the beneficial role of CNTs on mustard plant growth, have been documented.[17]

Given the absolute and increasing scale of production of nanomaterials allied to their uncertain effects on human health it is important that the presence of nanoparticles in the environment can be measured and monitored along with their chemical identification and concentration. The quantification of environmental nanoparticles represents a significant analytical challenge.[13] In the next section (8.2), we very briefly outline existing non-electrochemical methods before considering in detail electrochemical alternatives in Sect. 8.3.

## 8.2 Non-electrochemical Approaches to the Quantification of Environmental Nanoparticles and Their Limitations

The application of existing analytical methodology to the quantification of environmental nanoparticles has been summarised in an excellent review by Howard[13] who identifies the importance of techniques as follows: analyte enrichment (centrifugation, density gradient centrifugation, split-flow thin-cell fractionation); particle visualisation (scanning electron microscopy (SEM), transmission electron (TEM) and helium ion microscopy, atomic force microscopy); particle sizing in nanoparticle suspensions (disc centrifugation, nanoparticle tracking analysis, dynamic light scattering (DLS), UV-visible and fluorescence) and separation methods (flow cytometry, disc centrifuge, field-flow fractionation, hydrodynamic chromatography, size-exclusion chromatography, electrophoresis).

In comparison with the above, electrochemical methods are relatively underexplored but offer scope for chemical identification, low cost and ease of portability.

## 8.3 Electrochemical Approaches to the Quantification of Nanoparticles

### *8.3.1 Stripping Voltammetry of Nanoparticles*

The simplest approach to the electrochemical (voltammetric) analysis of nanoparticles is to first separate and isolate the nanoparticles from the sample of interest and then immobilise them on a suitable substrate electrode and conduct stripping voltammetric analysis. This approach can be illustrated by the elegant work of Giovanni and Pumera[18] on molybdenum metallic nanoparticle detection using cyclic and differential pulse voltammetry. They formed Mo nanoparticle-modified glassy carbon electrodes by depositing a small amount of colloidal suspension on the surface of a glassy carbon electrode and then letting the solvent (dimethylformamide) evaporate to dryness. Voltammograms were then recorded in phosphate buffer of neutral pH and these are shown in Fig. 8.1. Clearly defined oxidation features are discernible, fingerprinting the nanoparticles as Mo. A similar approach has been applied by the same group to Ni[19] and Ag[20] nanoparticles. Such analyses promise application in bioassays with the possibility that different nanoparticles can be used to label (tag) different species. For example CdS nanoparticles can be directly detected electrochemically in much the same way as Mo[21] and have been used to label DNA.[22]

In the case of Au nanoparticles a more indirect approach was taken.[23] First the Au nanoparticles were physically adsorbed of the surface of a glassy carbon electrode at open circuit. Subsequently electrochemical oxidation of the colloidal Au nanoparticles to $AuCl_4^-$ in 0.1 M aqueous HCl was carried out. Immediately

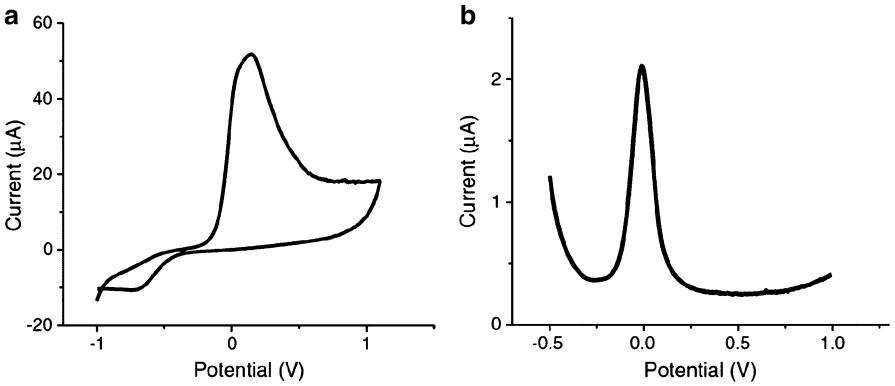


**Fig. 8.1** (**a**) Cyclic voltammogram for a glassy carbon electrode modified with 0.25 μg of molybdenum nanoparticles recorded in 50 mM phosphate buffer (pH 7.4) at a scan rate of 100 mV $s^{-1}$. (**b**) Differential pulse voltammetric response for the oxidation of 0.1 μg of molybdenum nanoparticles in 50 mM phosphate buffer (pH 7.4). Reprinted from reference (18) with permission from Elsevier

following this step the $AuCl_4^-$ formed was detected and quantified via differential pulse voltammetry.

There are several reports that the electrochemical oxidation of nanoparticles can be size dependent with both Ag[20,24] and Pt nanoparticles studied.[25] Ivanova and Zamborini immobilised different sized citrate-capped Ag nanoparticles ranging in size from 8 to 50 nm onto an amine-functionalised indium tin oxide (ITO)-coated glass electrode via electrostatic attachment to the protonated amine group. The largest diameter particles studied showed an oxidation potential in 0.1 M aqueous sulphuric acid ca. 100 mV more positive than that of the smallest nanoparticles studied.

The size dependency of the electrochemical oxidation of metal nanoparticles can be partially understood in the light of several different considerations.[24–30] First, data deriving from work on small silver clusters, $Ag_n$, formed in aqueous solution via pulse radiolysis coupled with other information such as mass spectroscopic equilibrium data and Gibbs energies of sublimation of silver has led to the estimation of the standard electrode potential of the redox couple

$$Ag_n \leftrightarrows Ag_{n-1} + Ag^+ + e^-$$

For large values of n the potential approaches that expected for the $Ag/Ag^+$ redox couple (+0.799 V). However at small values of n there is a strong size dependence[27] with a value of −1.8 V calculated for the special case of a single atom of silver (n = 1).[26–28] In between these limits the electrode potential varies as shown in Fig. 8.2 with a strong oscillation in the n = 1–3 range—the silver atom being strongly electron donating whereas the dimer (n = 2) is being almost "noble"[27] (−0.1 V) with the trimer again having a very negative value. The ease of oxidation of $Ag_n$ as n increases is evident in Fig. 8.2.

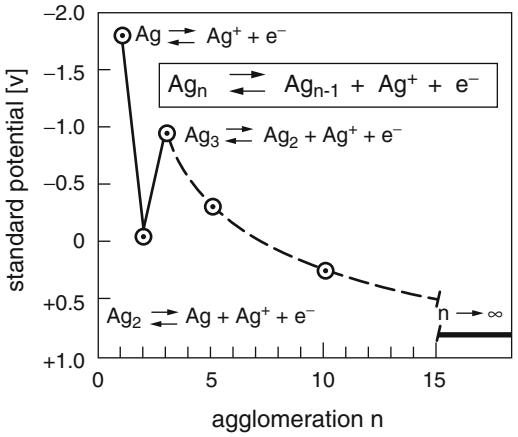


**Fig. 8.2** Variation of the standard electrode potential for the $Ag/Ag^+$ redox couple with agglomeration of silver atoms. Reprinted with permission from reference (27). Copyright 1993 American Chemical Society

For larger clusters approaching nanoparticle dimensions Plieth[26] considered surface Gibbs energies reflecting the fact that metal atoms in the surface of a small particle are in less energetically favourable positions compared to those in bulk material. He obtained the following equation for the difference in electrode potential between the dispersed (colloidal) metal as compared with the bulk material:

$$\Delta E \propto -\frac{\gamma}{r}$$

where the particles were considered to be spheres of radius r, γ is the surface energy ($J\ m^{-2}$) and the analysis was considered to apply to particles of ca 0.7 nm or larger in radius (corresponding to 100 atoms or so). Application of the theory required knowledge of surface energy values and this limited the application of the theory in real systems. Figure 8.3 however shows the results of some model calculations[26] and that significant shifts of redox potential can be seen for particles as large as 10 nm.

Developing from this type of approach Tang and colleagues[25] used first principle electronic structure calculations of the surface energy of Pt nanoparticles to develop size-dependent potential pH diagrams and to show, supported by experimental electrochemical scanning tunnelling microscopy, that Pt nanoparticles of diameter less than ~4 nm dissolve oxidatively via the direct electrochemical dissolution:

$$Pt \rightarrow Pt^{2+} + 2e^-$$

whereas larger nanoparticles form oxide layers.

A further consideration pertaining to size-dependent electrochemical oxidation of metal nanoparticles supported on a conductive electrode surface relates to the size-dependent concentration profiles of the metal ions produced during oxidation as they diffuse away from the electrode surface.[29–31] In order to identify the effects

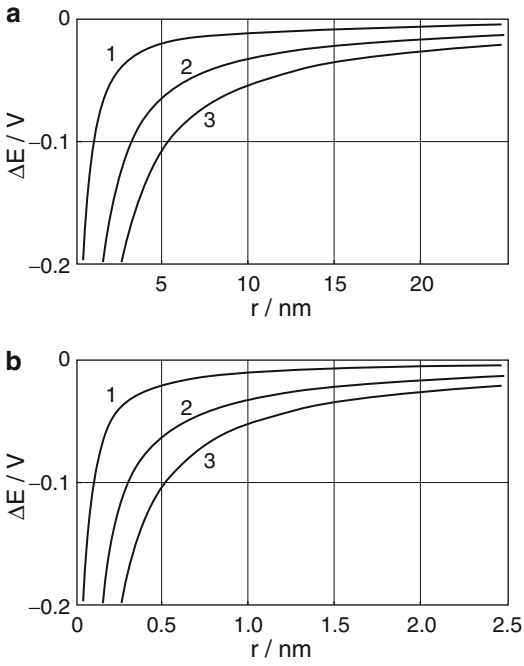


**Fig. 8.3** Cathodic shift in redox potential for a metal electrode as a function of particle size (**a**) particle radius $r < 25$ nm, (**b**) particle radius $r < 2.5$ nm for surface energy values of 0.5 J $m^{-2}$ (*curve 1*), 1.5 J $m^{-2}$ (*curve 2*) and 2.5 J $m^{-2}$ (*curve 3*). Adapted with permission from reference (26). Copyright 1982 American Chemical Society

of diffusion on the voltammetric stripping signal from an electrode partially covered with the nanoparticles (of a uniform size) being stripped, the formal potential for the oxidation was assumed constant in simulations made to isolate the effects of diffusion.[29–31] Under these conditions theory predicts that for electrochemically irreversible kinetics (slow electron transfer requiring an overpotential) the peak potential will be independent of the metal coverage but will shift to more negative potentials as the nanoparticle radius shrinks in size. If a range of nanoparticle sizes is present then this is reflected by the broadening of the stripping peak as observed experimentally for Bi nanoparticles being stripped from the surface of a boron-doped diamond electrode.[31]

In contrast for an electrochemically reversible stripping process it is predicted, again assuming no influence of particle size on the standard electrode potential of the stripping process, that assuming the diffusion layers surrounding each nanoparticle overlap so as to produce overall planar diffusion of the stripped ions away from the electrode, the peak potential will depend on the total metal coverage but not the nanoparticle size. In the opposite limit, where the diffusion layers do not overlap particle size effects are predicted. Experiments reported[30] for the electrochemically reversible stripping of silver nanoparticles supported on a basal plane pyrolytic graphite electrode showed the expected dependence on the metal loading but not the particle size.

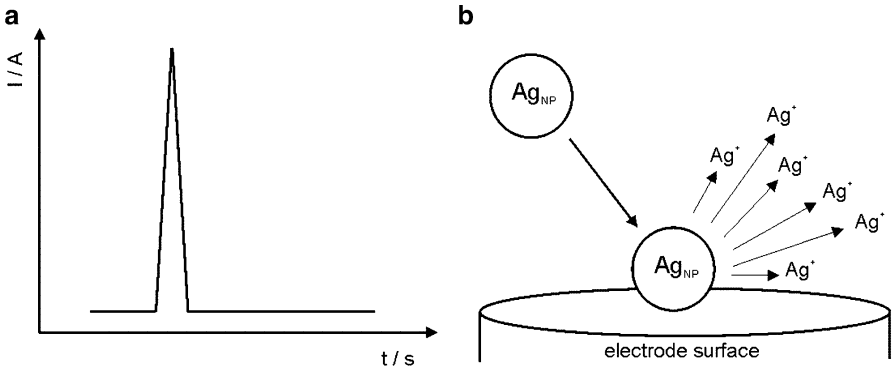


**Fig. 8.4** Schematic diagram of (**a**) the spike observed in the current-time transient when a silver nanoparticle collides with a potentiostated electrode and is oxidatively destroyed (**b**)

In summary, stripping voltammetry can be used to identify the presence of oxidisable nanoparticles, thus allowing fingerprinting and, with suitable calibration, their quantification although care is required in the interpretation of the peak potential with sensitivity to particle size and possible loadings.

### *8.3.2 Nanoparticle: Electrode Impacts*

An alternative and at least in principle much simpler and easier electrochemical approach to that of the previous section, in which nanoparticles are sequentially isolated, immobilised on an electrode and then analysed via stripping voltammetry, is the direct study of the nanoparticles suspended in a solution phase into which an electrode under potentiostatic control is introduced. The movement of the nanoparticles in the solution is expected to approximate to Brownian which from time to time will bring the nanoparticles close to or in physical contact with the electrode to which they can either stick or rebound, unless the electrode is held at a potential corresponding to the oxidation or reduction of the nanoparticles or at least the surface of the nanoparticles. In the latter case, the nanoparticle impacts on the electrode are revealed by a pulse of current, as shown schematically in Fig. 8.4. These spikes can be used to identify ("fingerprint") the nanoparticles (by virtue of their "onset potentials"), measure their concentrations and to size them as discussed in more detail below. This type of measurement is currently subject to significant levels of interest (see reference (32) for an early review).

The original work in the area was carried out by Heyrovský and colleagues[33–36] using mercury electrodes to electro-*reduce* particles of metal oxides. They examined the voltammetry of polydisperse "colloidal" solutions of the oxides $SnO_2$, $TiO_2$ and $Fe_2O_3$ in aqueous solution. The voltammograms measured reflected the summation of the contribution of groups of particles of different sizes and they were able[36] to

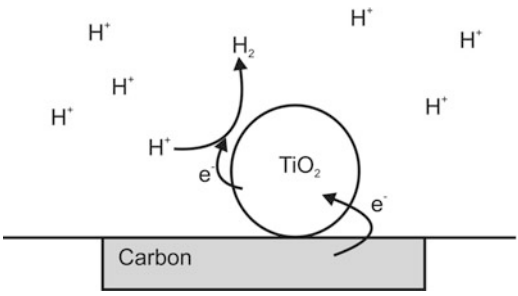


**Fig. 8.5** The indirect nanoimpact process studied by Heyrovský et al. in reference (35) where protons are reduced on the surface of impacting $TiO_2$ particles.[32] Adapted by permission of The Royal Society of Chemistry

voltammetrically determine the approximate composition of Fe(III)-doped $TiO_2$ colloids. The work was subsequently extended, again exclusively with mercury electrodes, to the reduction of oxide layers on the surfaces of "metal powders" (Cu, Fe, Ni, Mo, W),[37] on copper/copper oxide "ultrafine powders"[38] and finally on aluminium "nanoparticles".[39] In 35 the authors report the reduction of protons in acid solutions occurring on the surface of $TiO_2$ particles for the duration of their impacts with the electrode surface. This experiment is the forerunner of the "indirect processes" now studied more widely (see below and Fig. 8.5).

Innovative experiments were carried out by Scholz[40] in which the range of impact experiments were usefully extended to study the collisions of liposomes with a mercury electrode in aqueous solution at pH 7. Sharp current transients, of ca. 1–20 ms duration, were seen as the liposomes contacted, broke up and then spread over the electrode surface. However, unlike the experiments of Heyrovský, the current spikes were deduced to be non-faradaic in character with capacitative origins: the frequency of the transient signals was found to be a minimum at the potential of zero charge, pzc, and to increase with potentials negative or positive of the pzc. In subsequent work the kinetics of liposome adhesion were explored and also the impact of montmorillonite clay particles on a mercury electrode was studied.[41,42]

Related experiments were carried out by present authors' group using suspensions of oil droplets and solid particles in aqueous solutions induced into motion by power ultrasound and allowed to impact solid electrodes (Au, Pt).[43–46] Current transients of microsecond duration were seen corresponding to the much faster speed of the impacting particles as compared to those in the Scholz experiments, leading to a greatly reduced contact time between particle and electrode. The amount of charge passed in the impact transients scaled with the size and conductivity of the impacting particle and the sign of the current transient inverted at the pzc of the substrate electrode as shown in Fig. 8.6. Charge transfer between the particle and the electrode and/or the deformed double layer and the electrode was inferred but at the microsecond timescales resulting from insonation it was concluded that faradaic charge transfer was not operative and experiments using large insonated metal particles confirmed no such activity.

A significant advance was made in which similar experiments were performed using silver nanoparticles, $Ag_n$, but without insonation, rather using natural Brownian

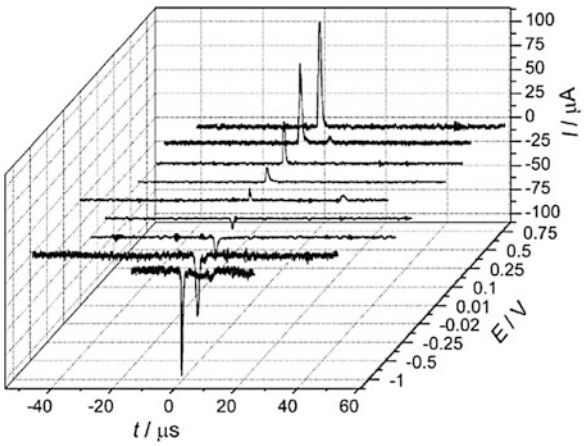


**Fig. 8.6** Current spikes observed for graphite powder (diameter 2–20 µm) impacting a gold microdisc electrode under sonication in 0.1 M perchloric acid. Reprinted with permission from reference (45). Copyright 2004 American Chemical Society

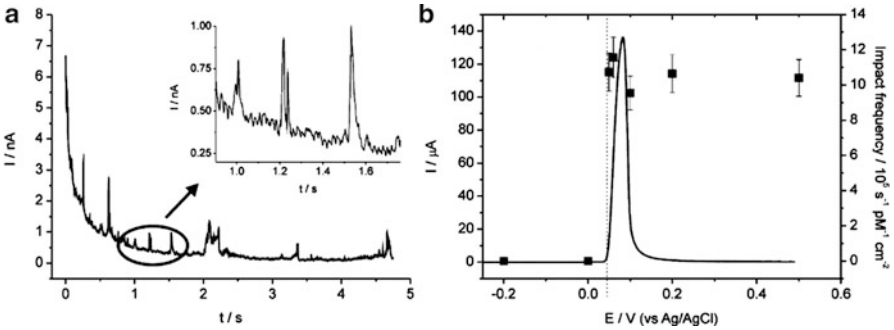


**Fig. 8.7** (**a**) Impact spikes observed when silver nanoparticles are directly oxidised upon collision with a potentiostated carbon microelectrode surface in 10 mM citrate/90 mM KCl. (**b**) Stripping voltammogram for a silver nanoparticle-modified glassy carbon electrode in 10 mM citrate/90 mM KCl (*left* axis) overlaid with the observed frequency of nano-impacts (*right* axis) at a carbon microelectrode in the same solution at varying potentials. Reproduced from reference (47). Copyright © 2013 WILEY-VCH Verlag GmbH & Co. KGaA, Weinhem

motion to give rise to the impact with an electrode surface.[47,48] Using a carbon electrode it was found that sharp current spikes of ca. 1–10 ms durations were seen (Fig. 8.7) when the electrode was potentiostatted at a value more positive than that required for the process in which the nanoparticles were oxidised to aqueous silver cations:

$$Ag_n - ne^- \rightarrow nAg^+(aq)$$

The onset potential for the observation of the spikes corresponded closely to the peak potential recorded if the same Ag nanoparticles were immobilised on a glassy carbon electrode (as in Sect. 8.3.1 above) and subjected to anodic stripping analysis (Fig. 8.7b). Furthermore, in the former experiments the frequency of the measured

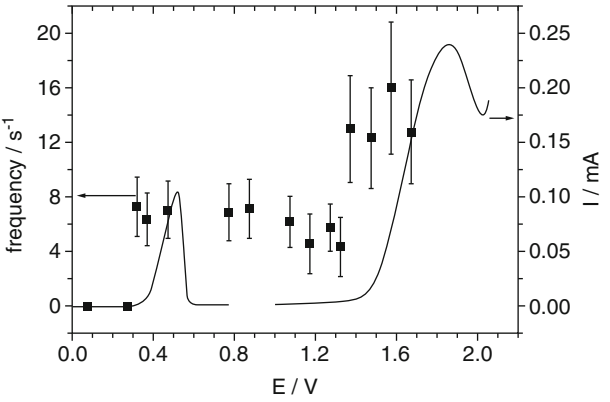


**Fig. 8.8** Overlay plot of stripping voltammetry for a glassy carbon electrode modified with silver (peak potential = +0.5 V) and nickel nanoparticles (peak potential = +1.8 V) with impact frequency of the nanoparticle mixture at a carbon microelectrode in 10 mM $HClO_4$/100 mM $NaClO_4$. The onset potential of spikes at 0.3 V corresponds to the direct oxidation of silver nanoparticles whilst the later switch on potential (+1.4 V) is caused by the mixed nanoparticles.[53] Reproduced by permission of The Royal Society of Chemistry

impacts scaled with the nanoparticle concentration in solution. Analogous experiments were conducted for the electro-oxidation of diverse other metal nanoparticles: gold,[49] copper[50] and nickel.[51,52] The different onset potential for the appearance of the oxidative spikes allowed mixtures of nanoparticles to be analysed, for example, mixtures of silver and nickel nanoparticles[53] as shown in Fig. 8.8.

It is evident that such experiments can provide information about the chemical identity of the impacting nanoparticles by virtue of the onset potential for the appearance of oxidative spikes. However it was additionally discovered that the oxidation of the nanoparticles is quantitative, so that all of the atoms in a particle become oxidised on impact even for a large nanoparticle of 100 nm in diameter.[47,48] This was understood in terms of a model[54] explicitly invoking Brownian motion interpreting the observed millisecond timescale current "spikes" as each resulting from a cluster of very rapidly consecutive encounters of the nanoparticle with the electrode, in each of which partial oxidation of the nanoparticle takes place, but such as to bring about the overall complete oxidation of the nanoparticle. Calculations suggested that it was unlikely that partially oxidised nanoparticles would survive on the observed millisecond timescale. It follows that the charge passed during the current spikes was directly and quantitatively linked with the number of atoms in the nanoparticles (Faraday's first law of electrolysis!) and hence with the nanoparticle size. Figure 8.9 shows the size distribution for nickel nanoparticles determined via oxidative electrode impacts ("anodic particle coulometry", APC) and that measured from SEM[53] where the nanoparticle radius has been inferred from the charge passed under the spikes on the assumption that the particle is spherical. Excellent and quantitative agreement is apparent.

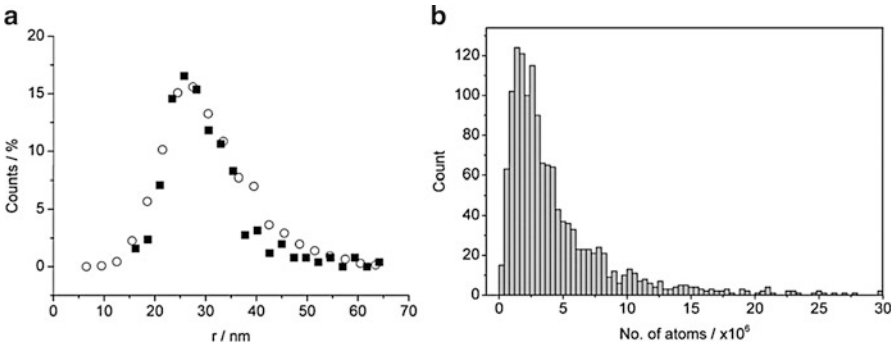


**Fig. 8.9** (**a**) Size distribution for nickel nanoparticles determined via anodic particle coulometry (*open circle*) overlaid with a distribution for the same nanoparticles determined using SEM (*filled square*). A radius (r) of approximately 26 nm is inferred. (**b**) Size distribution for nickel nanoparticles in terms of the number of atoms making up each nanoparticle colliding with the electrode surface.[53] Reproduced by permission of The Royal Society of Chemistry

The nickel nanoparticles used in the experiments[53] to generate Fig. 8.9 did not undergo any significant aggregation on the timescale of the voltammetric measurements. This is in contrast to silver and gold nanoparticles where it was found that the electrochemical measurements revealed the presence of aggregation in solution.[48,49] Figure 8.10 shows the atom counting and sizing for gold nanoparticles measured in 0.1 M aqueous HCl solution. The nanoparticles were sized as 20 nm in diameter via SEM; the electrochemistry shows the presence of some single nanoparticles (radius $10.5 \pm 0.5$ nm) as well as clusters of two or more nanoparticles,[49] thus revealing the occurrence of aggregation of the nanoparticles in aqueous solution. Similar observations were made for silver nanoparticles.[48] Thus APC allows not only particle sizing (number of atoms, radius of the nanoparticle if assumed spherical) but also, in principle, the extent and rate of nanoparticle aggregation in real time.

A detailed study was performed to investigate the capabilities of APC for nanoparticle agglomeration studies.[55] Agglomeration of silver nanoparticles in a citrate/potassium chloride solution was monitored by sizing the nanoparticles, in terms of the number of atoms contained in each silver nanoparticle, using APC. The analysis performed on the APC data took into consideration the link between the underlying normal distribution of a silver nanoparticle monomer and its agglomerates, ensuring that no physical meaning was lost during data fitting. In addition, nanoparticle tracking analysis (NTA), a commercially available nanoparticle-sizing device, was used to provide a critical comparison of the nanoparticle sizing results gained via APC.

As shown in Fig. 8.11, an excellent agreement was achieved between the two sizing techniques; moreover the electrochemical sizing technique was found to present a number of advantages over NTA, which can suffer from drawbacks commonly associated with optical sizing techniques such as the inability to measure the agglomeration state of non-spherical nanoparticles without performing a

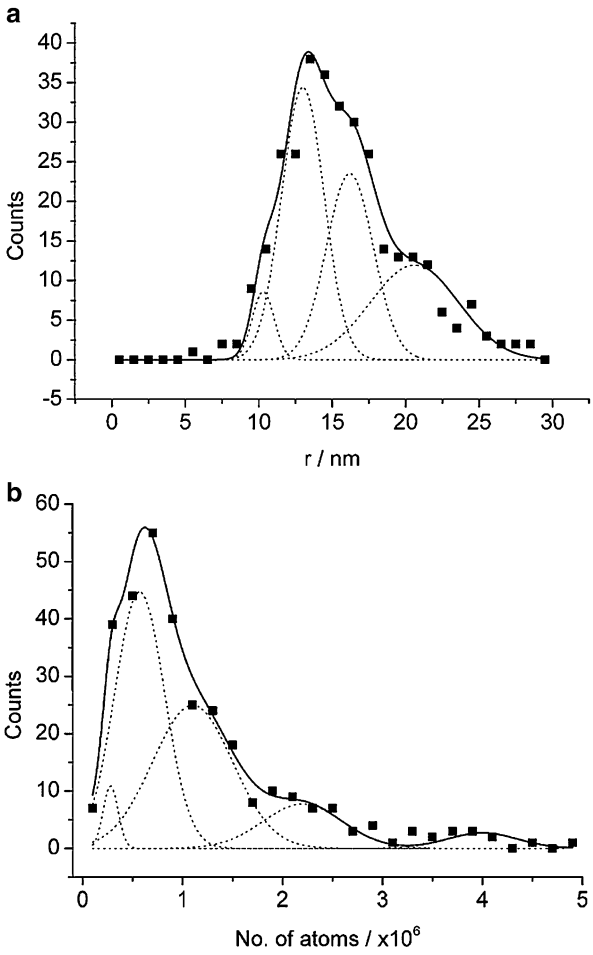


**Fig. 8.10** Size distribution for APC measurements of gold nanoparticles expressed as (**a**) radius (r) and (**b**) the number of atoms in an impacting nanoparticle.[49] Reproduced by permission of The Royal Society of Chemistry

correction as well as having limited application to nanoparticles contained in non-transparent solutions. A further study performed by our group found that it is possible to successfully achieve a slower rate of silver nanoparticle agglomeration/aggregation for a range of different sized particles when a high concentration of trisodium citrate is selected as the electrolyte thanks to its nanoparticle-stabilising properties.[56]

With the APC method having been shown to be effective for the detection and sizing of a variety of metal nanoparticles, an obvious progression of this work and the earlier work performed by Heyrovský[33–36] was to test the application of cathodic particle coulometry (CPC) for the detection of metal oxides. $Fe_3O_4$ nanoparticles were detected and sized using CPC with SEM employed to confirm the accuracy of this electrochemical sizing method.[57] Furthermore, it was discovered that using both CPC and APC in conjunction with one another (Fig. 8.12)

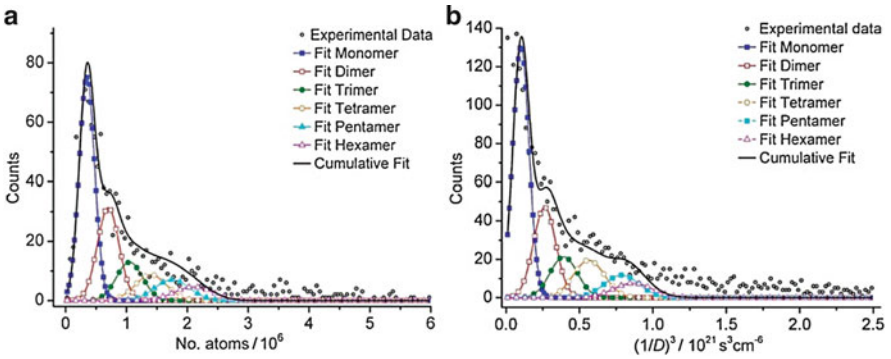


**Fig. 8.11** Distribution of silver nanoparticle size in 10 mM citrate/90 mM KCl detected by (**a**) APC and (**b**) NTA. The individual Gaussian distributions for nanoparticle monomers (*filled square*), dimers (*open square*), trimers (*filled circle*), tetramers (*open circle*), pentamers (*filled triangle*) and hexamers (*open triangle*) are overlaid to achieve the overall data fit (*continuous line*). Reproduced from reference (55). Copyright © 2013. The Authors. ChemistryOpen published by WILEY-VCH Verlag GmbH & Co. KGaA, Weinheim. This is an open-access article under the terms of the Creative Commons Attribution Non-Commercial License, which permits use, distribution and reproduction in any medium, provided the original work is properly cited and is not used for commercial purposes

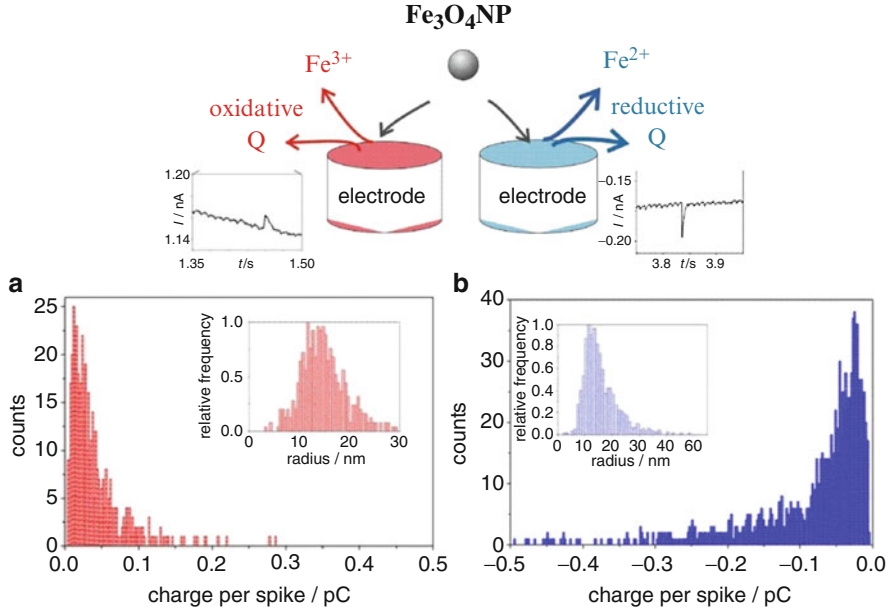


**Fig. 8.12** Schematic for the two electrochemical routes used to size $Fe_3O_4$ nanoparticles and the resulting charge and size (*inset*) distributions gained from (**a**) APC experiments and (**b**) CPC experiments. Reproduced from reference (57). Copyright © 2013 Tsinghua University Press and Springer-Verlag Berlin Heidelberg

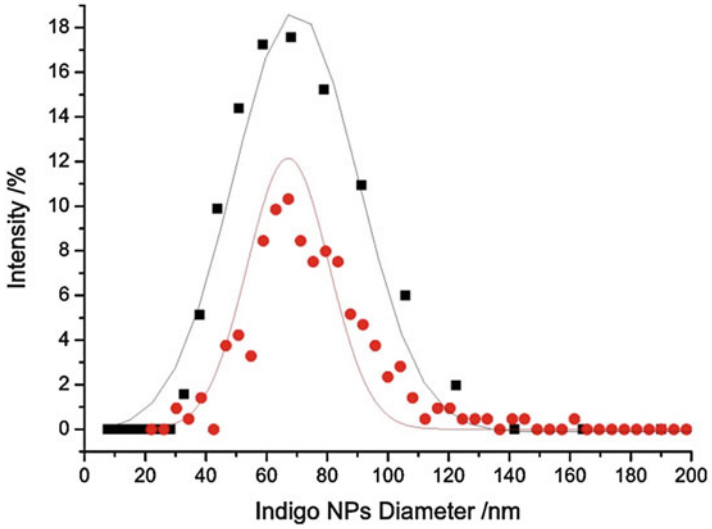


**Fig. 8.13** Overlaid distributions for indigo nanoparticle sizing measured via CPC (*filled circle*) and DLS (*filled square*). Reproduced from reference (58). Copyright © 2013 WILEY-VCH Verlag GmbH & Co. KGaA, Weinheim

provides a suitably accurate and thorough nanoparticle characterisation method, rendering the use of optical techniques for verification of these electrochemical sizing methods redundant.

One type of nanoparticles that are particularly difficult to size using currently available techniques is organic nanoparticles. Experiments were conducted to investigate the suitability of CPC as an alternative to existing techniques (e.g. SEM, TEM, DLS, ultracentrifugation) used for organic nanoparticle sizing, with indigo nanoparticles used as a model system.[58] Figure 8.13 shows the size distribution gained for the electro-reduction of indigo nanoparticles via CPC in comparison with the size analysis of the same batch of nanoparticles determined using DLS. It can be seen that the resulting size distributions from both techniques are in excellent agreement, with a mean diameter of the indigo nanoparticles investigated being 68 nm.

The viability of the impact approach has been demonstrated in authentic seawater media. Figure 8.14a shows oxidative current-time transients of citrate-capped silver nanoparticles ($13 \pm 2$ nm in radius) dispersed in seawater measured at a carbon microelectrode of radius ca. 6 μm[59] whilst Fig. 8.14b shows the size distribution of the nanoparticles in terms of the number of atoms making up each nanoparticle inferred from the charge passed during transients such as those in Fig. 8.14a. From the independently measured average nanoparticle size of 13 nm radius it can be estimated that a single silver nanoparticle of this size contains ca. $5.4 \times 10^5$ atoms. It is evident from Fig. 8.14 that the nanoparticles must be extensively aggregated in the seawater (on the timescale studied which was ca. 40 min from the addition of the nanoparticles); deconvolution of the distribution

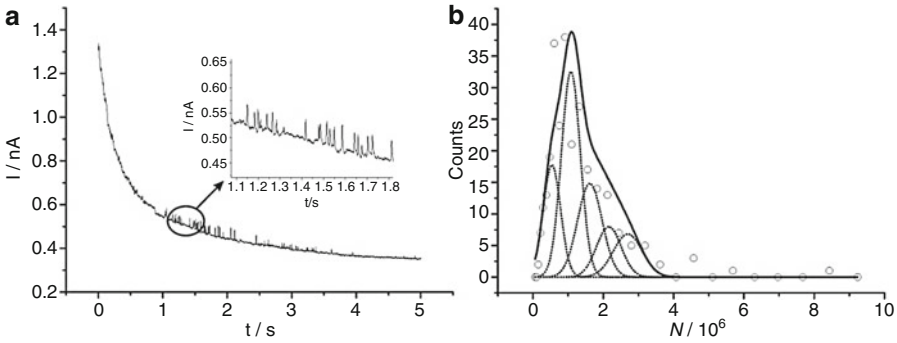


**Fig. 8.14** (**a**) Oxidative impact spikes for silver nanoparticles in authentic seawater media. (**b**) Size distribution for silver nanoparticles in seawater obtained via APC expressed as the number of atoms ($N$) per impacting nanoparticle and deconvoluted to reveal contributions from aggregates.[59] Reproduced (**a**) and adapted (**b**) by permission of The Royal Society of Chemistry

in Fig. 8.14b suggested significant contributions from not only single nanoparticles but also aggregates of 2, 3, 4 and 5 nanoparticles corresponding to $1.08 \times 10^6$, $1.62 \times 10^6$, $2.16 \times 10^6$ and $2.70 \times 10^6$ atoms, respectively.

The types of nanoparticles used for APC/CPC experiments have either been synthesised in-house (Ag, Au) or purchased directly from chemical companies (Cu, $Fe_3O_4$). With the number of nanoparticle-based products available to purchase on the market increasing, it is typically the nanoparticles contained in these products that are leaching into the environment and posing a risk to the ecosystem. Therefore, it is these nanoparticles in consumer goods for which the need for effective detection and characterisation techniques suitable for use in the field is great. As a result, one such product, a colloidal silver disinfectant spray, was selected to determine if the nanoparticles contained within it could be studied using APC.[60] It was found that APC was effective at successfully detecting and sizing the silver nanoparticles contained in the disinfectant spray in both a standard electrolyte solution ($radius_{NP} = 11$ nm) and seawater ($radius_{NP} = 10.3$ nm). Figure 8.15 shows the size distributions achieved via APC and NTA methods and the excellent agreement between the two for both solutions in which the nanoparticles were dispersed.

In addition to particle identification and sizing, the impact method can also be used to measure the concentration of nanoparticles in solution. This is best done by measuring oxidative impacts at a micro-disc electrode, typically made of carbon. The current (I)-time transient at such an electrode following the application of a potential sufficient to oxidise species under diffusion control in an n-electron process is

$$I = 4nFCDr_e f(\tau)$$

where F is the Faraday constant, C is the bulk concentration of the electroactive species, D is the diffusion coefficient of the latter and $f(\tau)$ is a dimensionless time.

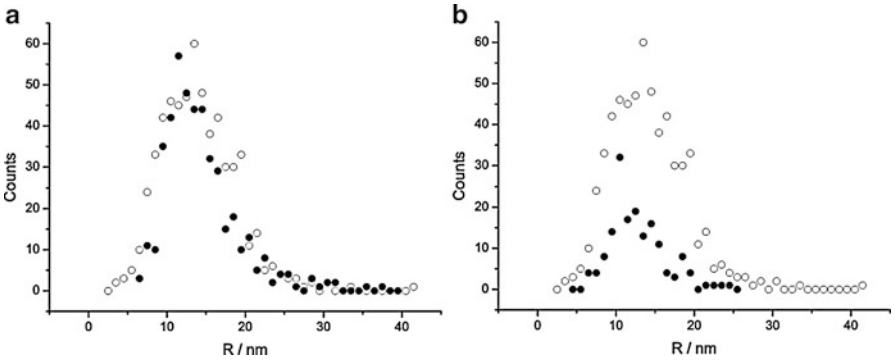


**Fig. 8.15** Size distributions for the radius (R) of silver nanoparticles contained in a commercially available disinfectant cleaning spray determined via NTA (*open circle*) and APC (*filled circle*) in (**a**) 0.1 M $NaClO_4$ and (**b**) authentic seawater media. Reproduced from reference (60)

The latter is defined by $\tau = 4Dt/r_e^2$ where $r_e$ is the microdisc radius and t is time. This expression is very well established for molecular species where the form of $f(\tau)$ has been given by Shoup and Szabo[61] where at short times the flux to the electrode surface is linear and a Cottrellian transient behaviour is seen where $I \alpha Cr_e^2(D/t)^{1/2}$ whilst for longer times, where convergent diffusion is established, $f \rightarrow 1$ so that $I \alpha Cr_eD$. The implication of the differing dependences on D in the limiting forms is that if measurements are made to span the timescales of both linear and convergent diffusion then fitting of the transient allows the separate determination of the terms (nC) and D. In the molecular context, it follows that if one of n or C is known then both the unknown parameter (n or C) and D can be found via the measurement of a potential step chronoamperometric transient. The power of this approach is well documented allowing, in effect, coulometry (the measurement of n) on the voltammetric timescale without the need for exhaustive electrolysis as pertains at macro-sized electrodes.[62]

In the context of nano-impact data such as that in Fig. 8.7a it is best expressed as a plot of the cumulative number of impacts as a function of time. This can then be compared with an integrated form of the Shoup-Szabo expression.[53] Fitting the latter to the former so as to determine C, the unknown concentration of nanoparticles, requires a knowledge of $r_e$ (which can be found by independent electrochemical calibration) and D, the nanoparticle diffusion coefficient. Given the large size of the nanoparticles the latter can be reliably calculated from the Stokes-Einstein equation

$$D = \frac{k_B T}{6\pi\eta r_{np}}$$

where $r_{np}$ is the radius of the nanoparticle, $k_B$ is the Boltzmann constant and $\eta$ is the solvent viscosity. Note that this approach is inappropriate for molecules because they are too small to reliably use the Stokes-Einstein equation. In the case of nanoparticles, $r_{np}$ can be reliably determined from the APC experiment as noted above.

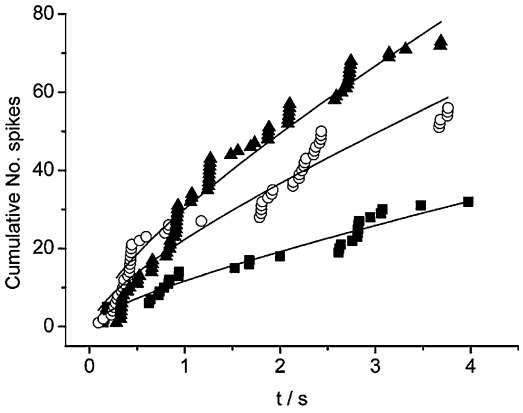


**Fig. 8.16** Fitting the accumulative number of spikes as a function of time with an integrated form of the Shoup-Szabo expression for a nanoimpact experiment using varying concentrations of nickel nanoparticles, (*filled square*) 28 pM, (*open circle*) 54 pM and (*filled triangle*) 77 pM, in 10 mM $HClO_4$ and 100 mM $NaClO_4$.[53] Reproduced by permission of The Royal Society of Chemistry

Figure 8.16 shows data for the cumulative number of impacts versus time obtained for three different samples of Ni nanoparticles of known concentrations—$28 \pm 4$, $54 \pm 8$ and $77 \pm 11$ pM. The theoretical lines shown in the figure arise from the best fit of the integrated form of the Shoup and Szabo flux equation with the nanoparticle diffusion coefficient estimated by the Stokes-Einstein equation using the APC-determined value of $r_{np}$. The best fit concentration values were 30, 60 and 80 pM in excellent agreement with the known values, thus validating the use of nano-impacts as a means of measuring nanoparticle concentrations. The method was extended to systems in which aggregation was present.[53]

The above suggests the following general strategy for both sizing and measuring the unknown concentration of nanoparticles in a single experiment. First current–time transients are recorded—such as those in Fig. 8.7a)—and the data analysed first to give the average charge per "spike". The latter can, in the absence of aggregation, then be converted into a nanoparticle radius assuming that the nanoparticles are approximately spherical. With a knowledge of $r_{np}$, an estimate of the nanoparticle diffusion coefficient can be made from the Stokes-Einstein equation. The original data can then be converted into a plot of the cumulative number of impacts as a function of time and fitted using the integrated Shoup-Szabo equation and the estimated diffusion coefficient to give the sought unknown concentration. By way of caveat, it might be noted that this approach is approximate in the sense that it assumes that the nanoparticle diffusion coefficient is equivalent to that in the bulk solution at all points adjacent to the electrode. In practice, nanoparticles suffer "hindered diffusion" near solid surfaces,[63,64] with the local diffusion coefficient reduced below its bulk value; however this has been shown to have a relatively negligible effect on the analysis suggested.[65]

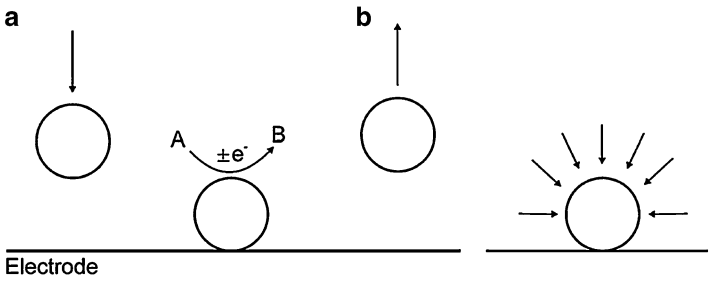


**Fig. 8.17** (**a**) Schematic of an indirect process involving a redox reaction occurring on the surface of the nanoparticle when it is in contact with the electrode. (**b**) Upon impact convergent diffusion to the nanoparticle occurs almost instantaneously meaning a steady-state current is established for the electrocatalytic reaction occurring on the nanoparticle surface. Reprinted from reference (68) with permission from Elsevier

The above impact experiments involve the exhaustive electro-oxidation of metal nanoparticles. An alternative non-destructive method for nanoparticle identification and sizing has been proposed[66,67] in which the surface of metal nanoparticles such as silver or gold is "tagged" by the adsorptive attachment of redox active molecules onto the surfaces of the nanoparticles. The tagged nanoparticles are allowed to impact an electrode surface just as in APC except that now the electrode potential is held at a value such as to reduce or oxidise the tag. Typical tags might contain nitrophenyl[66] or ferrocenyl groups which, respectively, undergo reduction or oxidation in aqueous media. Thiol groups can be used to anchor the tags on silver or gold nanoparticle surfaces. In the case where a full monolayer of tag covers the nanoparticle surfaces then the average charge passed under the "spikes" measured in an impact experiment provides information about the average surface area of the nanoparticles and hence, under the assumption that the particles are spherical, an indication of the nanoparticle size (radius). Radii inferred via this approach were in excellent agreement with those obtained for the same nanoparticles using APC.[67]

In the nano-impact experiments discussed to date the electron transfer to or from the nanoparticles is a direct transfer. It is worth noting that, building on Heyrovský's[35] observations of proton reduction on the surface of $TiO_2$ nanoparticles impacting mercury electrodes, considerable progress has been made on the study of "indirect" electron transfers. Figure 8.17 schematically shows the concept underlying this experiment. As before Brownian motion of nanoparticles brings them into contact with an electrode under potentiostatic control. Whilst a nanoparticle is in contact, usually for a period of 1–10 ms, it adopts the potential of the electrode so that if redox active molecules are present in solution they can undergo electrolysis on the surface of the nanoparticle. If the nanoparticle-electrode combination is carefully selected then at some potential values electrolysis can be exclusively confined to the nanoparticles. For the case of silver nanoparticles suspended in aqueous acid solution impacting a carbon electrode,[68] the reduction of protons on the impacting silver nanoparticles can be seen as current "spikes" at potentials less cathodic than needed for their reduction on the underlying carbon electrode.

The analysis of the potential dependence of the current spikes allows for the deduction of electron transfer kinetics of redox couples at single nanoparticles via appropriate modelling[51,68,69] treating the impacted nanoparticle as a sphere on a flat surface, and recognising that the time needed to set up steady-state electrolysis at the nanoparticle surface is tiny compared to the duration of the impacts so that the nanoparticle-confined electrolysis can be accurately treated as being at steady state. It should however be recognised that some nanoparticles can "stick" to the electrode surface which thus gradually changes its chemical (and electrochemical nature) over the course of time; values for the sticking probabilities have been measured.[70,71] Other chemical examples of these indirect processes are given by Bard in a review of his group's work in the area.[72] In the case of electrochemically irreversible processes the potentials needed to see the process taking place on the nanoparticles can be shifted to significantly higher potentials than required on macro-electrodes made of the corresponding material because of the much enhanced diffusional mass transport at the nanoscale, leading to a greater overpotential for the redox reaction of interest.[68]

Similar considerations, most notably treating the transport to an impacted sphere as being at steady state, also allow the modelling of the APC type of impact experiment where the nanoparticle is exhaustively oxidised and in particular the prediction of the onset potential for the appearance of current "spikes". Different behaviour is predicted for fast or slow (electrochemically reversible or irreversible) charge transfer kinetics.[50,52] Copper[50] and nickel[52] nanoparticles showed slow electron transfer kinetics whereas silver nanoparticles showed reversible kinetics.[52] The latter observation explains the fact that the onset potential for the appearance of oxidation "spikes" for the silver nanoparticles approximately matches the peak potential in the stripping voltammetry when the same particles are immobilised on an electrode.

### *8.3.3 Nanoparticle Detection at "Sticky" Surfaces*

For the application of the nanoparticle-electrode impact methods described in Sect. 8.3.2 to environmental monitoring one major drawback is that the environmental samples to be tested would have to be isolated and transported to a laboratory before the nanoparticles within the selected sample can be detected via APC/CPC. Here, the user would run the risk of the nanoparticles within the sample changing (e.g. aggregating) before analysis can be performed. Therefore, an in situ nanoparticle detection method is desirable for this type of field work. One such method is to immobilise nanoparticles in solution on an electrode surface under open-circuit conditions before oxidatively stripping off the nanoparticles using anodic stripping voltammetry to reveal the amount of nanoparticles that have adhered to the surface and therefore providing information on the concentration of nanoparticles in solution.[73] Again, the potential of the stripping peak can be used to identify the type of nanoparticles present.

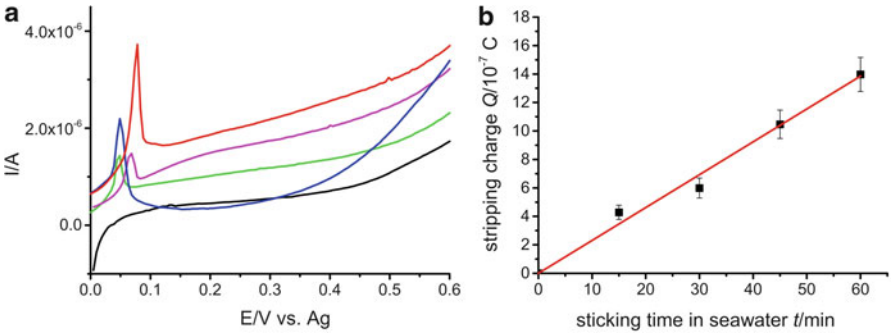


**Fig. 8.18** (**a**) Anodic stripping voltammograms for the oxidation of silver nanoparticles contained in a commercially available colloidal silver spray cleaning product that had become adhered to a screen-printed carbon electrode in authentic seawater media after 0 min (black line), 15 min (green line), 30 min (pink line), 45 min (blue line) and 60 min (red line). (**b**) A plot of the stripping charge for the silver nanoparticle stripping peaks vs. time. Reproduced from reference (74)

It is possible to increase the adhesion extent and rate of nanoparticle adsorption on the electrode surface by modifying the surface so that it becomes "sticky". The electrochemical modification of a glassy carbon electrode surface with cysteine was found to increase the ability of silver nanoparticles in 0.1 M $NaClO_4$ to stick onto the surface of the electrode, with larger stripping peaks observed at much shorter times in comparison to sticking experiments at an unmodified substrate.[73] Figure 8.18 shows how the same cysteine "sticky" electrodes were found to be suitable for the detection of silver nanoparticles contained in a commercially available colloidal silver disinfectant spray using disposable carbon electrodes immersed in authentic seawater media.[74]

## 8.4 Outlook

The study of nanoparticles is in its infancy and that is especially the case for the electrochemistry of these environmentally important species, where measurements can be expected to reveal important information about the redox behaviour of nanoparticles as well as provide analytical methods for their characterisation. That said, to date, voltammetric methods have been developed for the identification of nanoparticles as well as offering the possibility for sizing them, monitoring their aggregation in real time and measuring their concentrations. Already electrochemical methods are providing significant insights into the behaviour of naturally occurring environmental nanoparticles[75–79] and an explosion of growth in this area and related areas is to be expected in the near future.

## References


1. Duffus JH, Nordberg M, Templeton DM (2007) Glossary of terms used in toxicology, 2nd ed. Pure Appl Chem 79:1153–1344
2. Sanchez A, Recillas S, Font X, Casals E, Gonzalez E, Puntes V (2011) Ecotoxicity of, and remediation with, engineered inorganic nanoparticles in the environment. Trends Anal Chem 30:507–516
3. Chen Z, Yadghar AM, Zhao L, Mi Z (2011) A review of environmental effects and management of nanomaterials. Toxicol Environ Chem 93:1227–1250
4. Zanker H, Schierz A (2012) Engineered nanoparticles and their identification among natural nanoparticles. Annu Rev Anal Chem 5:107–132
5. Kumar P, Kumar A, Lead JR (2012) Nanoparticles in the Indian environment: known, unknowns and awareness. Environ Sci Technol 46:7071–7072
6. Karn B, Kuiken T, Otto M (2009) Nanotechnology and in situ remediation: a review of the benefits and potentials risks. Environ Health Perspect 117:1823–1831
7. Yavuz CT, Mayo JT, Yu WW, Prakash A, Falkner JC, Yean S, Cong L, Shipley HJ, Kan A, Tomson M, Natelson D, Colvin VL (2006) Low-field magnetic separation of monodisperse $Fe_3O_4$ nanocrystals. Science 314:964–969
8. Lisha KP, Pradeep T (2009) Towards a practical solution for removing inorganic mercury from drinking water using gold nanoparticles. Gold Bull 42:144–149
9. Dickinson M, Scott TB (2010) The application of zero-valent iron nanoparticles for the remediation of a uranium-contaminated waste effluent. J Hazard Mater 178:171–178
10. Xu YH, Zhao DY (2007) Reductive immobilization of chromate in water and soil using stabilized iron nanoparticles. Water Res 41:2101–2110
11. Üzüm Ç, Shahwan T, Eroğlu AE, Lieberwirth I, Scott TB, Hallam KR (2008) Application of zero-valent iron nanoparticles for the removal of aqueous $Co^{2+}$ ions under various experimental conditions. Chem Eng J 144:213–218
12. Glover RD, Miller JM, Hutchison JE (2011) Generation of metal nanoparticles from silver and copper objects: nanoparticle dynamics on surfaces and potentials sources of nanoparticles in the environment. ACS Nano 5:8950–8957
13. Howard AG (2010) On the challenge of quantifying man-made nanoparticles in the aquatic environment. J Environ Monit 12:135–142
14. Donaldson K, Stone V, Tran CL, Kreyling W, Borm PJ (2004) Nanotoxicology. Occup Environ Med 61:727–728
15. Moos PJ, Chung D, Woessner M, Honeggar M, Cutler NS, Veranth JM (2010) ZnO particulate matter requires cell contact for toxicity in human colon cancer cells. Chem Res Toxicol 23:733–739
16. Burello E, Worth AP (2010) A theoretical framework for predicting the oxidative stress potential of oxide nanoparticles. Nanotoxicology 5:228–235
17. Mondal M, Basu R, Das S, Nandy P (2011) Beneficial role of carbon nanotubes on mustard plant growth: an agricultural prospect. J Nanoparticle Res 13:4519–4528
18. Giovanni M, Pumera M (2011) Molybdenum metallic nanoparticle detection via differential pulse voltammetry. Electrochem Commun 13:203–204
19. Giovanni M, Ambrosi A, Pumera M (2012) The inherent electrochemistry of nickel/nickel-oxide nanoparticles. Chem Asian J 7:702–706
20. Giovanni M, Pumera M (2012) Size dependant electrochemical behaviour of silver nanoparticles with sizes of 10, 20, 40, 80 and 107 nm. Electroanalysis 24:615–617
21. Merkoçi A, Marcolino LH, Marin S, Fatibello-Filho O, Alegret S (2007) Detection of cadmium sulphide nanoparticles by using screen-printed electrodes and a handheld device. Nanotechnology 18:035502
22. Marin S, Merkoçi A (2009) Direct electrochemical stripping detection of cystic-fibrosis-related DNA linked through cadmium sulfide quantum dots. Nanotechnology 20:055101

23. Pumera M, Aldavert M, Mills C, Merkoçi A, Alegret S (2005) Direct voltammetric determination of gold nanoparticles using graphite-epoxy composite electrode. Electrochim Acta 50:3702–3707
24. Ivanova OS, Zamborini FP (2010) Size-dependent electrochemical oxidation of silver nanoparticles. J Am Chem Soc 132:70–72
25. Tang L, Li X, Cammarata RC, Friesen C, Sieradzki K (2010) Electrochemical stability of elemental metal nanoparticles. J Am Chem Soc 132:11722–11726
26. Plieth W (1982) Electrochemical properties of small clusters of metal atoms and their role in surface enhanced raman scattering. J Phys Chem 86:3166–3170
27. Henglein A (1993) Physicochemical properties of small metal particles in solution: "microelectrode" reactions, chemisorption, composite metal particles, and the atom-to-metal transition. J Phys Chem 97:5457–5471
28. Henglein A (1977) The reactivity of silver atoms in aqueous solutions (a γ-radiolysis study). Ber Bunsenges Phys Chem 81:556–561
29. Ward Jones SE, Chevallier FG, Paddon CA, Compton RG (2007) General theory of cathodic and anodic stripping voltammetry at solid electrodes: mathematical modelling and numeral simulations. Anal Chem 79:4110–4119
30. Ward Jones SE, Campbell FW, Baron R, Xiao L, Compton RG (2008) Particle size and surface coverage effects in the stripping voltammetry of silver nanoparticles: theory and experiment. J Phys Chem C 112:17820–17827
31. Ward Jones SE, Toghill KE, Zheng SH, Morin S, Compton RG (2009) The stripping voltammetry of hemispherical deposits under electrochemically irreversible conditions: a comparison of the stripping voltammetry of bismuth on boron-doped diamond and Au(III) electrodes. J Phys Chem C 113:2846–2854
32. Rees NV, Zhou Y-G, Compton RG (2012) Making contact: charge transfer during particle-electrode collision. RSC Adv 2:379–384
33. Heyrovský M, Jirkovský J (1995) Polarography and voltammetry of ultrasmall colloids: introduction to a new field. Langmuir 11:4288–4292
34. Heyrovský M, Jirkovský J, Müller BR (1995) Polarography and voltammetry of aqueous colloidal $SnO_2$ solutions. Langmuir 11:4293–4299
35. Heyrovský M, Jirkovský J, Štruplová-Bartáčková M (1995) Polarography and voltammetry of aqueous colloidal $TiO_2$ solutions. Langmuir 11:4300–4308
36. Heyrovský M, Jirkovský J, Štruplová-Bartáčková M (1995) Polarography and voltammetry of mixed titanium(IV) oxide/iron(III) oxide colloids. Langmuir 11:4309–4312
37. Korshunov AV, Heyrovský M (2006) Voltammetry of metallic powder suspensions on mercury electrodes. Electroanalysis 18:423–426
38. Korshunov A, Heyrovský M (2009) Electrochemical behaviour of copper metal core/oxide shall ultra-fine particles on mercury electrodes in aqueous dispersions. J Electroanal Chem 629:23–29
39. Korshunov A, Heyrovský M (2010) Voltammetry of aluminium nanoparticles in aqueous media with hanging mercury drop electrode. Electroanalysis 22:1989–1993
40. Hellberg D, Scholz F, Schauer F, Weitschies W (2002) Bursting and spreading of liposomes on the surface of a static mercury drop electrode. Electrochem Commun 4:305–309
41. Scholz F, Hellberg D, Harnisch F, Hummel A, Hasse U (2004) Detection of the adhesion events of dispersed single montmorillonite particles at a static mercury drop electrode. Electrochem Commun 6:929
42. Hellberg D, Scholz F, Schubert F, Lovrioć M, Omanović D, Hernández VA, Thede R (2005) Kinetics of liposome adhesion on a mercury electrode. J Phys Chem B 109:14715–14726
43. Banks CE, Rees NV, Compton RG (2002) Sonoelectrochemistry in acoustically emulsified media. J Electroanal Chem 535:41–47
44. Banks CE, Rees NV, Compton RG (2002) Sonoelectrochemistry understood via nanosecond voltammetry: sono-emulsions and the measurement of the potential of zero charge of a solid electrode. J Phys Chem B 106:5810–5813

45. Rees NV, Banks CE, Compton RG (2004) Ultrafast chronoamperometry of acoustically agitated solid particulate suspensions: nonFaradaic and Faradaic processes at a polycrystalline gold electrode. J Phys Chem B 108:18391–18394
46. Clegg AD, Rees NV, Banks CE, Compton RG (2006) Ultrafast chronoamperometry of single impact events in acoustically agitated solid particulate suspensions. ChemPhysChem 7:807–811
47. Zhou Y-G, Rees NV, Compton RG (2011) The electrochemical detection and characterization of silver nanoparticle in aqueous solutions. Angew Chem Int Ed 50:4219–4221
48. Rees NV, Zhou Y-G, Compton RG (2011) The aggregation of silver nanoparticles in aqueous solution investigated via anodic particle coulometry. ChemPhysChem 12:1645–1647
49. Zhou Y-G, Rees NV, Pillay J, Tshikhudo R, Vilakazi S, Compton RG (2012) Gold nanoparticles show electroactivity: counting and sorting nanoparticles upon impact with electrodes. Chem Commun 48:224–226
50. Haddou B, Rees NV, Compton RG (2012) Nanoparticle-electrode impacts: the oxidation of copper nanoparticles has slow kinetics. Phys Chem Chem Phys 14:13612–13617
51. Zhou Y-G, Rees NV, Compton RG (2013) Electrochemistry of nickel nanoparticles is controlled by surface oxide layers. Phys Chem Chem Phys 15:761–763
52. Zhou Y-G, Haddou B, Rees NV, Compton RG (2012) The charge transfer kinetics of the oxidation of silver and nickel nanoparticles via particle-electrode impact electrochemistry. Phys Chem Chem Phys 14:14354–14357
53. Stuart EJE, Zhou Y-G, Rees NV, Compton RG (2012) Determining unknown concentrations of nanoparticles: the particle-impact electrochemistry of nickel and silver. RSC Adv 2:6879–6884
54. Dickinson EJF, Rees NV, Compton RG (2012) Nanoparticle-electrode collision studies: brownian motion and the timescale of nanoparticle oxidation. Chem Phys Lett 528:44–48
55. Ellison J, Tschulik K, Stuart EJE, Jurkschat K, Omanović D, Uhlemann M, Crossley A, Compton RG (2013) Get more out of your data: a new approach to agglomeration and aggregation studies using nanoparticle impact experiments. ChemistryOpen 2:69–75
56. Lees JC, Ellison J, Batchelor-McAuley C, Tschulik K, Damm C, Omanović D, Compton RG (2013) Nanoparticle impacts show high-ionic-strength citrate avoids aggregation of silver nanoparticles. ChemPhysChem 14:3895–3897
57. Tschulik K, Haddou B, Omanović D, Rees NV, Compton RG (2013) Coulometric sizing of nanoparticles: cathodic and anodic impact experiments open two independent routes to electrochemical sizing of $Fe_3O_4$ nanoparticles. NanoResearch 6:836–841
58. Cheng W, Zhou X-F, Compton RG (2013) Electrochemical sizing of organic nanoparticles. Angew Chem Int Ed 52:12980–12982
59. Stuart EJE, Rees NV, Cullen JT, Compton RG (2013) Direct electrochemical detection and sizing of silver nanoparticles in seawater media. Nanoscale 5:174–177
60. Stuart EJE, Tschulik K, Omanović D, Cullen JT, Jurkschat K, Crossley A, Compton RG (2013) Electrochemical detection of commercial silver nanoparticles: identification, sizing and detection in environmental media. Nanotechnology 24:444002
61. Shoup D, Szabo A (1982) Chronoamperometric currents at finite disk electrode. J Electroanal Chem 140:237–245
62. Paddon CA, Bhatti FL, Donohoe TJ, Compton RG (2006) Cryo-electrochemistry in tetrahydrofuran: the electrochemical reduction of a phenyl thioether: [(3-{[*trans*-4-(Methoxymethoxy)cyclohexyl]oxy}propyl)thio]benzene. J Electroanal Chem 589:187–194
63. Brenner H (1961) The slow motion of a sphere through a viscous fluid towards a plane surface. Chem Eng Sci 16:242–251
64. Bevan MA, Prieve DC (2000) Hindered diffusion of colloidal particles very near to a wall: revisited. J Chem Phys 113:1228–1236
65. Barnes EO, Compton RG (2013) The rate of adsorption of nanoparticles on microelectrode surfaces. J Electroanal Chem 693:73–78

66. Zhou Y-G, Rees NV, Compton RG (2012) The electrochemical detection of tagged nanoparticles via particle-electrode collisions: nanoelectroanalysis beyond immobilisation. Chem Commun 48:2510–2512
67. Rees NV, Zhou Y-G, Compton RG (2012) The non-destructive sizing of nanoparticles via particle-electrode collision: tag-redox coulometry (TRC). Chem Phys Lett 525:69–71
68. Kahk JM, Rees NV, Pillay J, Tschikhudo R, Vilakazi S, Compton RG (2012) Electron transfer kinetics at single nanoparticles. Nano Today 7:174–179
69. Ward KR, Lawrence NS, Hartshorne RS, Compton RG (2012) Modelling the steady state voltammetry of a single spherical nanoparticle on a surface. J Electroanal Chem 683:37–42
70. Zhou Y-G, Rees NV, Compton RG (2011) Electrode-nanoparticle collisions: the measurement of the sticking coefficient of silver nanoparticles on a glassy carbon electrode. Chem Phys Lett 514:291–293
71. Zhou Y-G, Stuart EJE, Pillay J, Vilakazi S, Tshikhudo R, Rees NV, Compton RG (2012) Electrode-nanoparticle collisions: the measurement of the sticking coefficients of gold and nickel nanoparticles from aqueous solution onto a carbon electrode. Chem Phys Lett 551:68–71
72. Bard AJ, Zhou H, Kwon SJ (2010) Electrochemistry of single nanoparticles via electrocatalytic amplification. Israel J Chem 50:267–276
73. Tschulik K, Palgrave R, Batchelor-McAuley C, Compton RG (2013) 'Sticky electrodes' for the detection of silver nanoparticles. Nanotechnology 24:295502
74. Cheng W, Stuart EJE, Tschulik K, Compton RG (2013) A disposable sticky electrode for the detection of commercial silver nanoparticles in seawater. Nanotechnology 24:505501
75. Bura-Nakić E, Krznarić D, Helz GR, Ciglenečki I (2012) Characterization of iron sulfide species in model solutions by cyclic voltammetry. Revisiting an old problem. Electroanalysis 23:1376–1382
76. Bura-Nakić E, Viollier E, Jézéquel D, Thiam A, Ciglenečki I (2009) Reduced sulfur and iron species in anoxic water column of meromictic crater Lake Pavin (Massif Central, France). Chem Geol 266:311–317
77. Helz GR, Ciglenečki I, Krznarić D, Bura-Nakić E (2011) Voltammetry of sulphide nanoparticles and the FeS(aq) problem. Aquat Redox Chem 1071:265–282
78. Krznarić D, Helz GR, Bura-Nakić E, Jurašin D (2008) Accumulation mechanism for metal chalcogenide nanoparticles at $Hg^0$ electrodes; Cu sulfide example. Anal Chem 80:742–749
79. Bura-Nakić E, Krznarić D, Jurašin D, Helz GR, Ciglenečki I (2007) Voltammetric characterization of metal sulfide particles and nanoparticles in model solutions and natural waters. Anal Chim Acta 594:44–51